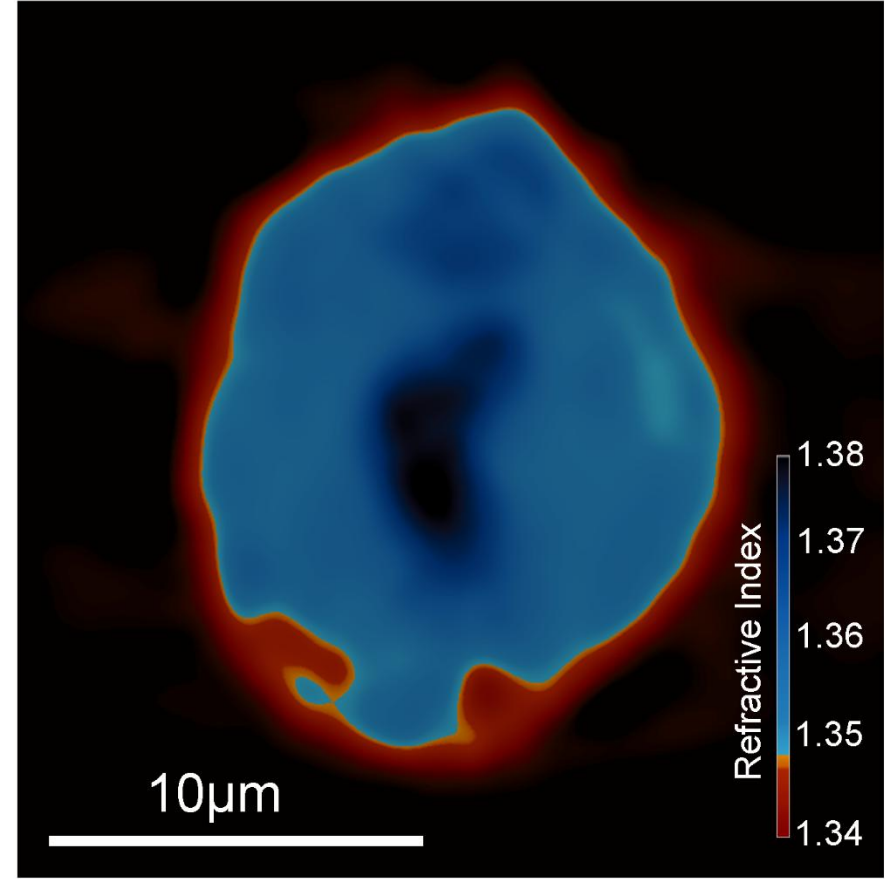




Introduction

- The volumetric distribution of the refractive index (RI) in cells is linked to biologically relevant structures in their interior [1].
- RI tomography enables the recovery of 3D RI distributions in inhomogeneous specimens such as biological cells.
- RI tomography is based on quantitative phase imaging (QPI) techniques and requires a set of measurements under varying viewing conditions.
- QPI enables label-free imaging of phase (transparent) specimens.
- Here, we demonstrate video-rate QPI of a HEK cell and RI tomography using coded wavefront sensing (Coded WFS).
- The performance is benchmarked against the well-established digital holographic microscopy (DHM) method.

Fig. 1: 2D HEK cell slice.



Intracellular Matter	Refractive Index
Cytosol	1.360 – 1.390
Nucleus	1.355 – 0.365
Nucleolus	1.375 – 1.385
Mitochondria	1.400 – 1.420

Coded Wavefront Sensing

- The phase mask introduces random delays to the reference and object waves, creating two speckle patterns, $I_0(\mathbf{r})$ and $I(\mathbf{r})$.
- The relationship underpinning the motion of the pixels in the speckle patterns is leveraged to retrieve the amplitude A and phase ϕ [2]:

$$\min_{\phi, A} \left\| I\left(\mathbf{r} + \frac{z}{k} \Delta\phi\right) - |\tilde{A}|^2 I_0(\mathbf{r}) \right\|_2^2 + \Gamma(\phi) + \Gamma(A)$$

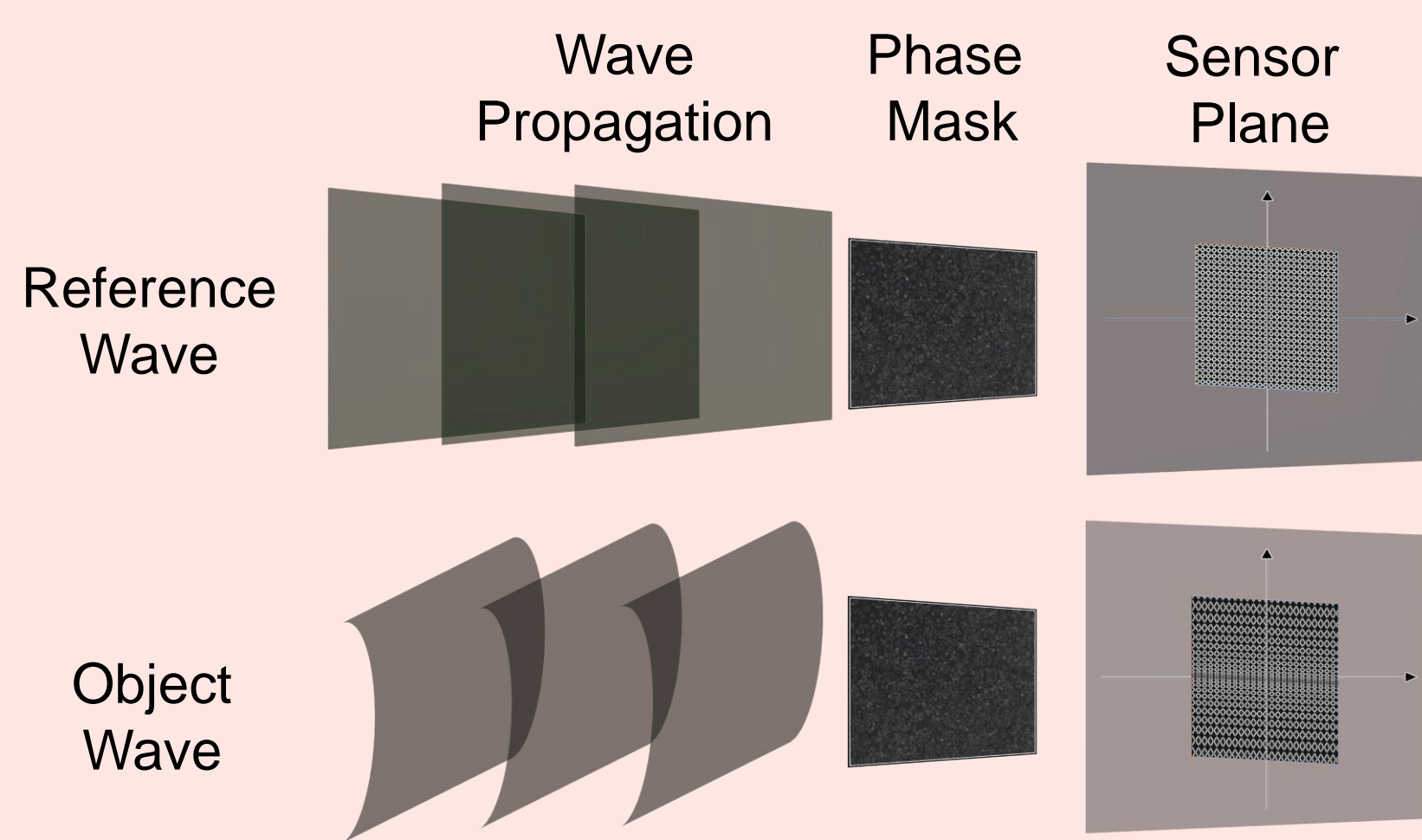


Fig. 2: Working principle of Coded WFS. Reference and object waves are captured by the sensor in the absence and presence of the specimen, respectively.

Coded WFS offers:

- Single-shot phase retrieval using computational imaging techniques.
- Direct integration with standard microscopes.
- Less stringent hardware, calibration, and expertise requirements.
- Less/no coherence artifacts.

Digital Holographic Microscopy

- DHM is a well-established, single-shot phase retrieval technique, considered to produce ground-truth phases in this work.
 - In DHM, a tilted reference wave R interferes with the object wave $O = Ae^{i\phi}$ in the sensor/hologram plane.
 - Due to the interference of the coherent waves, the sensor records an image I ,
- $$I = (O + R)(O + R)^* = \|O\|_2^2 + \|R\|_2^2 + OR^* + O^*R.$$
- This enables amplitude and phase recovery of the specimen, O .

Validation Using Cell Cluster Phantom

- Identical models of HeLa cells, with RI of 1.55 at 633 nm and maximum height of 8.4 μm , are placed in different orientations to form a cluster.
- The designed cell phantom and measured phantom (using DHM and Coded-WFS) OPD maps, including errors between them, are demonstrated below:

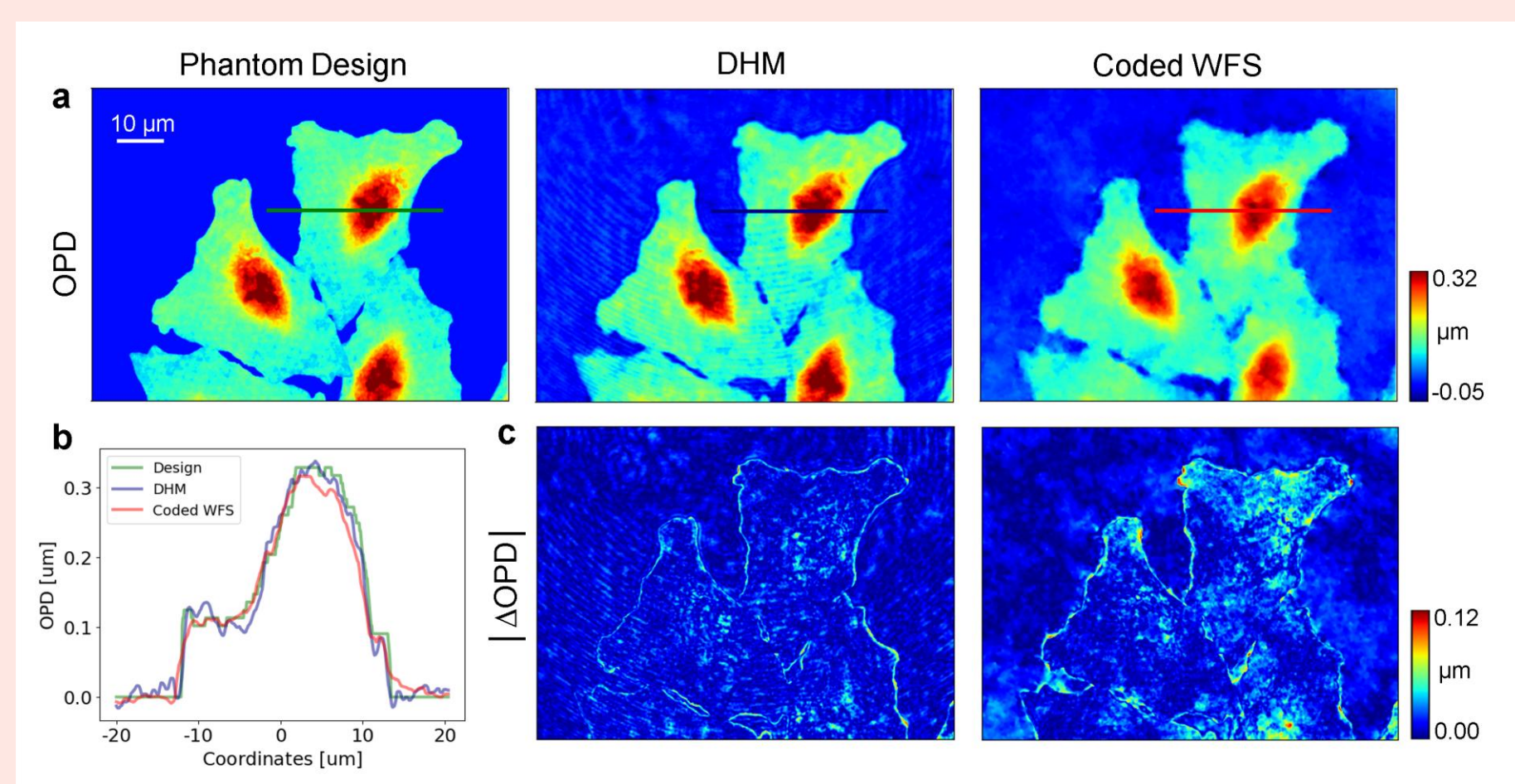


Fig. 3: Performance validation using a 3D-printed cluster of artificial HeLa cells.

References

- P. Y. Liu, L. K. Chin, W. Ser, et al., "Cell refractive index for cell biology and disease diagnosis: Past, present and future," Lab on a Chip 16, 634–644 (2016).
- C. Wang, Q. Fu, X. Dun, and W. Heidrich, "Quantitative phase and intensity microscopy using snapshot white light wavefront sensing," Sci. Reports 9, 13795 (2019).
- M. K. Løvmo, S. Moser, G. Thalhammer-Thurner, and M. Ritsch-Marte, "Acoustofluidic trapping device for high-NA multi-angle imaging," Front. Phys. 10, 940115 (2022).
- S. M. Kazim, et al., "Coded wavefront sensing for video-rate quantitative phase imaging and tomography: validation with digital holographic microscopy," Opt. Express (Accepted) (2025).

Experimental Setup

- DHM and Coded WFS are installed on two separate observation ports of a commercial inverted light microscope.
- The setup enables measurement of specimens by the two methods in quick succession under identical settings.
- The light scattered by the specimen is collected by an objective lens (40 \times NA 1.15, water immersion).
- The acoustofluidic trapping device [3] is mounted on the microscope stage to trap and rotate individual fixated HEK 293 cells, used for recording phase videos and tomography.

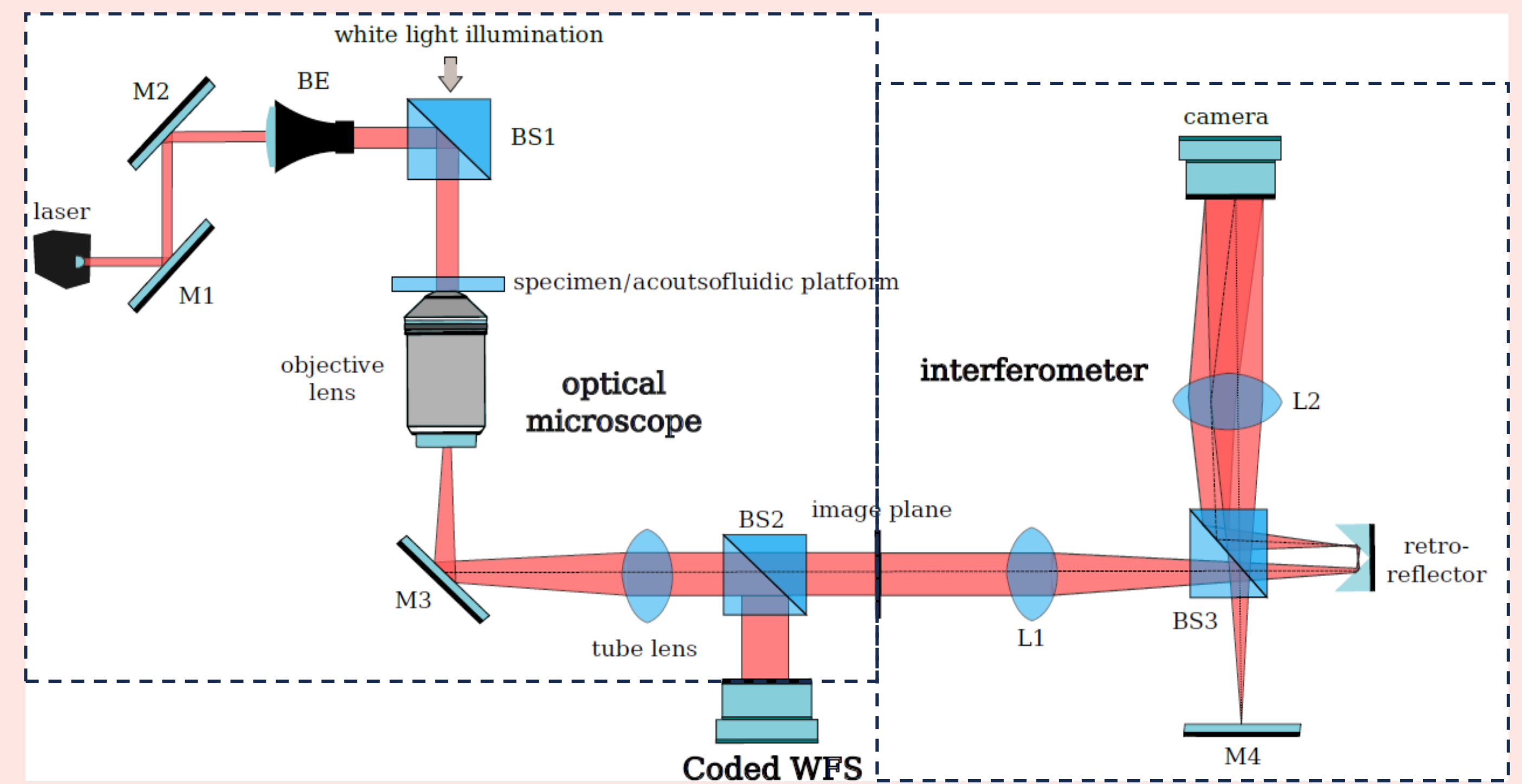


Fig. 4: Experimental setup. The sample is mounted on a commercial inverted microscope (Nikon ECLIPSE Ti2-E) and separately illuminated by two sources: A fibre-coupled diode laser for DHM and a broadband LED for Coded WFS. The two output ports of the microscope are operated sequentially for dynamic measurements. M, mirror; BE, beam expander; BS, beam splitter; L, lens.

Results: Video-Rate Phase Reconstruction

- A single HEK cell is trapped and actuated using the acoustofluidic trapping device.
- The cell rotates about an axis orthogonal to the imaging axis at $\approx 0.39 \text{ rad s}^{-1}$.
- The same HEK cell rotating with the same periodicity is recorded successfully by each system in succession.
- Coded WFS retrieves clear brightfield intensity images while DHM suffers from diffraction artifacts.
- The spatial resolution of the DHM reconstructions is observed to be qualitatively better than Coded WFS.
- In both methods, the temporal resolution is only limited by the camera hardware.
- The experimental setup provides unimpeded access to 360° of viewing angles about one (or more) object axis.

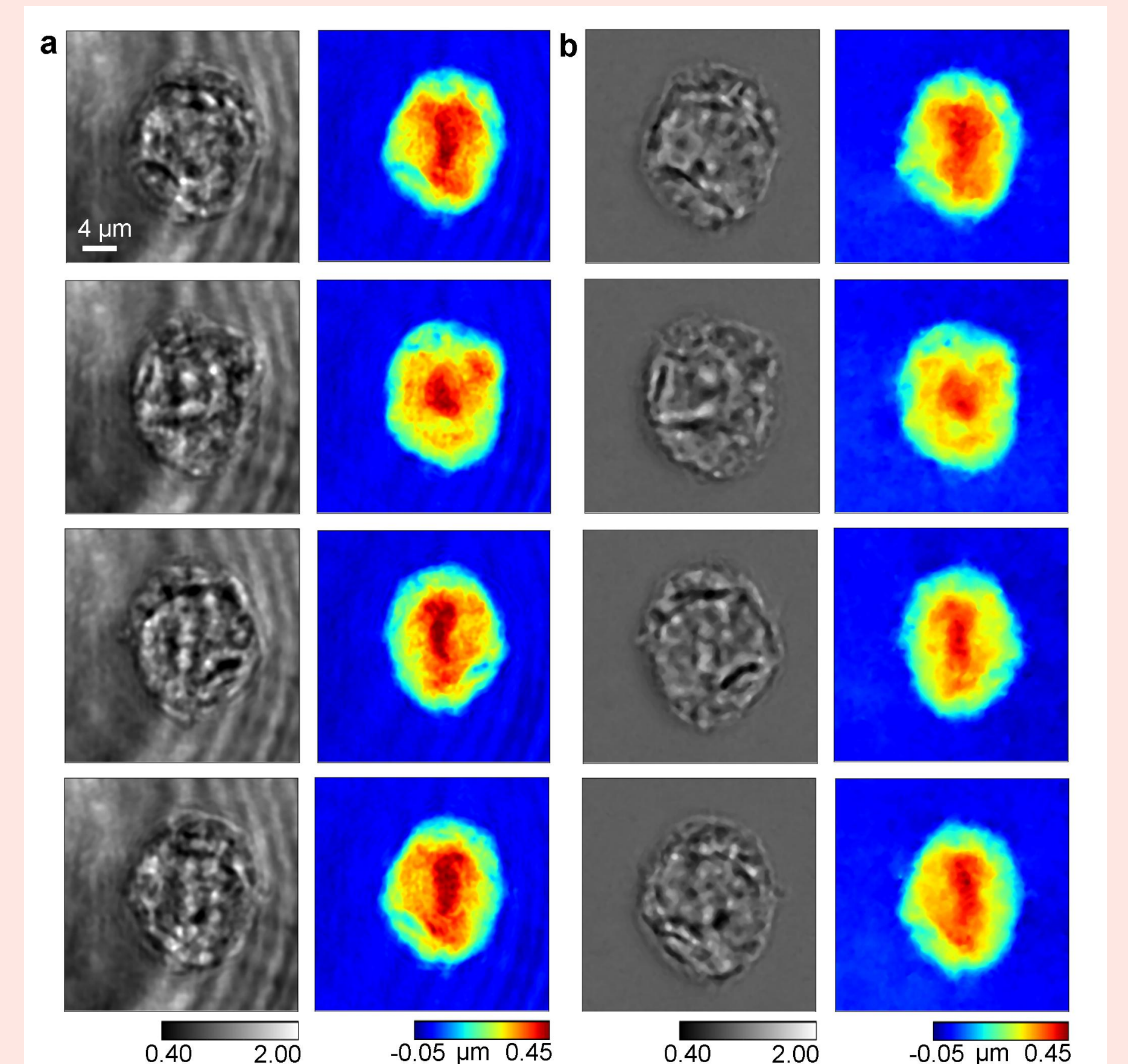


Fig. 5: Video-rate ($\approx 30 \text{ fps}$) QPI. Quantitative reconstructions of intensity (left) and OPD (right) of corresponding frames using a DHM and b Coded WFS of a rotating HEK293 cell.

Results: Refractive Index Tomography

- We treat each OPD as a projection of the 3D RI distribution corresponding to a pose (angle of rotation).
- Using the Fourier diffraction theorem, 2D spectra of the OPD projections can be mapped to semi-spherical surfaces in the 3D spectrum of the specimen.
- The center of each mapping is dependent on the pose information.
- The semi-spherical surfaces within the low-pass filtered frequency support are approximately linear planes.
- Therefore, we apply the simpler Fourier slice theorem to reconstruct the 3D RI distribution of the HEK cell [4].

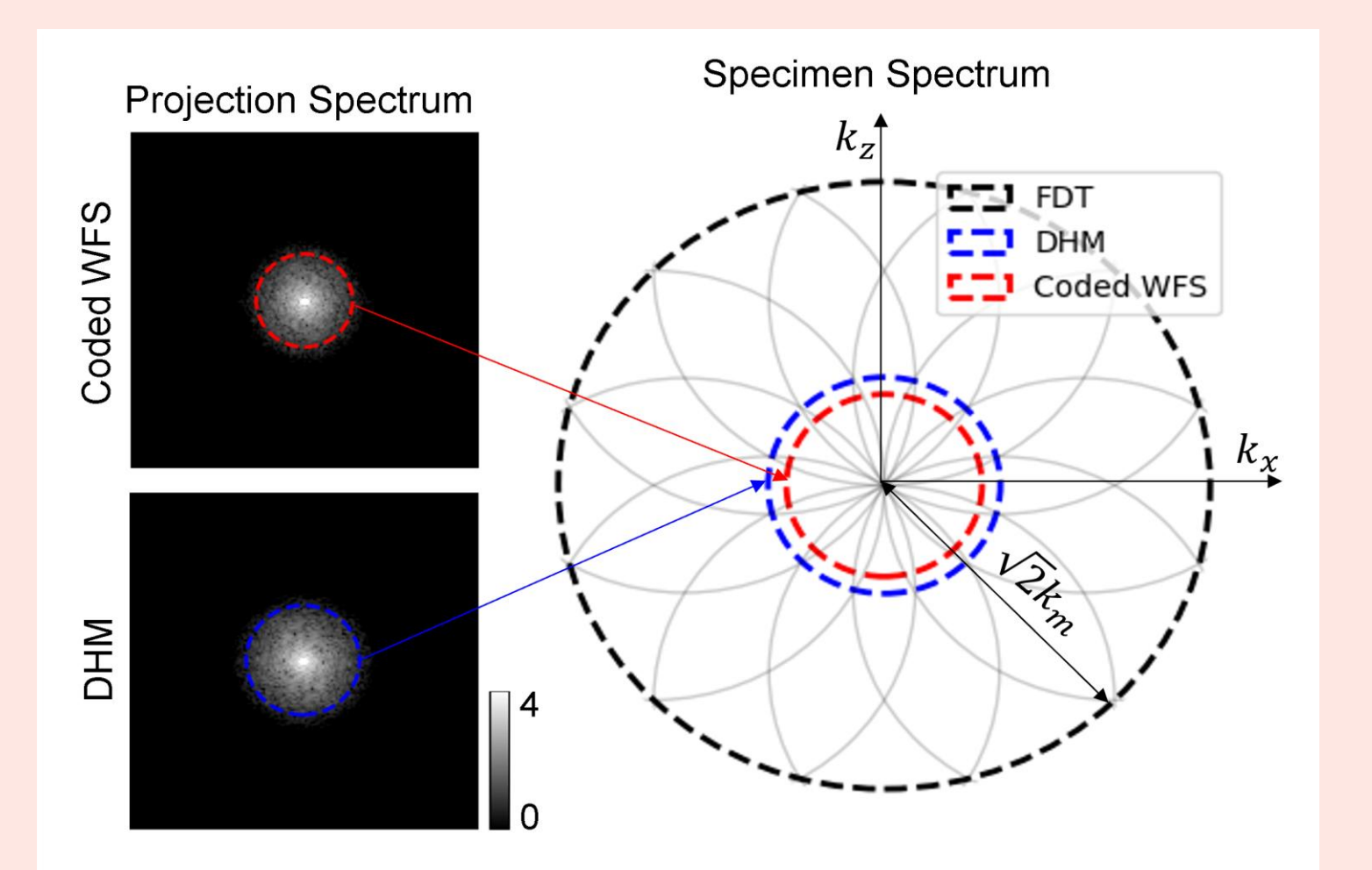


Fig. 6: Mapping projection spectrum to specimen spectrum. The magnitudes of the spectra [log -space] of the spatially smoothed phases (left) are mapped to the spectrum of the specimen (right).

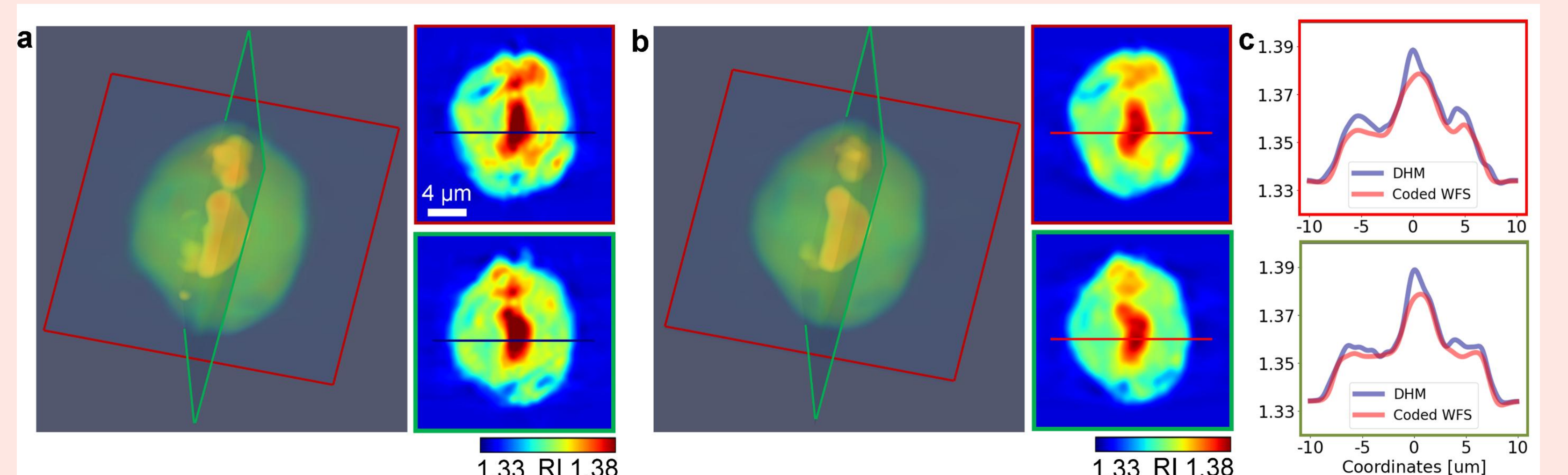


Fig. 7: 3D RI estimation. 3D RI distribution (left) and two slices (right) corresponding to the planes in the 3D visualization of a HEK293 cell estimated using 360°-view OPDs retrieved by a DHM and b Coded WFS. c The red and green-bordered RI line profiles from the similarly bordered RI slices in a and b.